

## FINITE ELEMENT INELASTIC ANALYSIS OF 3-D FLEXIBLE PAVEMENTS UNDER MOVING LOADS

Niki D. Beskou<sup>1</sup>, George D. Hatzigeorgiou<sup>2</sup> and Dimitrios D. Theodorakopoulos<sup>3</sup>

<sup>1</sup>Department of Civil Engineering  
University of Patras  
Patras, GR-26500, Greece  
e-mail: [nikidiane@gmail.com](mailto:nikidiane@gmail.com)

<sup>2</sup>School of Sciences and Technology  
Hellenic Open University  
Patras, GR-26335, Greece  
e-mail: [hatzigeorgiou@eap.gr](mailto:hatzigeorgiou@eap.gr)

<sup>3</sup>Department of Civil Engineering  
University of Patras  
Patras, GR-26500, Greece  
e-mail: [d.d.theod@upatras.gr](mailto:d.d.theod@upatras.gr)

**Keywords:** Flexible Pavements, Moving Loads, Inelastic Layers, Finite Elements.

**Abstract.** *The dynamic response of flexible road pavements to moving vehicles is numerically obtained by the time domain finite element method under three-dimensional conditions. The pavement is modeled as a layered finite rectangular domain. The material behavior of the layers is assumed to be inelastic: viscoelastic or viscoplastic for the top asphalt layer and elastic or elastoplastic of the von Mises and the Prager-Drucker type, respectively, for the other layers. The moving with constant speed loads (wheels) of the vehicle are simulated by assigning time dependent load values at all the surface nodes along the vehicle path, which are activated at the time it takes for every load to travel the distance from the origin to every node's location. Distributed moving loads are considered. Simple supports on rollers for the bottom and lateral boundaries of the pavement domain are assumed. Comparisons with corresponding elastic solutions are made in order to assess the inelastic material behavior on the response of the pavement.*

### 1 INTRODUCTION

Analytical and experimental research on the analysis and design of flexible pavements has attracted the attention of many investigators during the last 35 years or so [1-3]. Originally, flexible pavements were modeled as layered systems exhibiting linear elastic material behavior and subjected to static, stationary, distributed load. Then the load was assumed stationary but dynamic (impact load) to simulate the test process of deflectometry. Even though elastic flexible pavements under static load can be analysed approximately by hand, for realistic boundary conditions and dynamic and/or moving loads, use of numerical methods, such as the finite element method (FEM) is imperative [4].

Linear elastic material behavior is obviously an approximation and if one requires analytic results close to experimental ones, he has to adopt inelastic material behavior. Use of linear viscoelastic material behavior for the top asphalt layer, while retaining all the other layers linear elastic, certainly improved the results [5-7] but there was still a difference of 15% between them and the tests. Further improvements were achieved by using

viscoelastic material behavior for the top layer and non-linear elastic one for the other layers. This non-linear elastic behavior was simulated by stress-dependent moduli and use of iterations [1, 8-14]. In almost all of the above cases use was made of the FEM under two-dimensional (2-D) or three-dimensional (3-D) conditions and the load was assumed to be stationary and static with the exception of references [13], where the load is moving and [14], where the load is stationary but dynamic (impact load).

A more rational way to describe non-linear material properties is by using theories of plasticity and viscoplasticity. Thus, Zaghoul and White [15] assumed linear viscoelastic material behavior for the top layer and elastoplastic one of Drucker-Prager and Cam-Clay types for the base and subgrade layers, while Sukumaran et al [16] elastic material behavior for the top layer and elastoplastic one of the Mohr-Coulomb type for the other layers. In [15, 16] use was made of the 3-D FEM and the loads were assumed to be moving ones with constant speed. Saad et al [17], Fang et al [18] and Ali et al [19] also considered non-linear behavior of the layers: viscoplastic in all layers in [17], viscoplastic in the top layers and Drucker-Prager elastoplastic in the other layers in [19] and elastic in the top layer and Drucker-Prager and Cam Clay in the other layers in [18]. In [17-19] use was made of 2-D and 3-D FEM and the loads were assumed to be quasi-static ones. This last assumption about the loads reduces the size of the domain and allows a more detailed modeling of the wheel loads of the vehicle [17].

In this work, a 3-D finite element methodology is developed with the aid of the commercial software ANSYS [20] for the determination of the time domain response of three layered flexible pavements to moving loads on their surface. The asphalt concrete top layer is modeled as a viscoelastic or viscoplastic material, while the other two layers (base and subgrade) are modeled as elastic or elastoplastic (von Mises or Drucker-Prager) materials, respectively. It should be noted here that the term 'inelastic' is used in this work (title and text) in the broad sense of not including purely elastic behavior and in that sense includes viscoelastic behavior. Simple supports on rollers are used at the bottom and the lateral faces of the domain because, as it was found in [4] for the elastic case, this kind of supports for the size of the domain and its discretization in [4] provides results of the same accuracy with those obtained using absorbing viscous boundaries.

The wheel loads of the vehicle are assumed in this work to be distributed constant in magnitude loads moving with constant speed. They are simulated by assigning time dependent load values at all the surface nodes along the vehicle path, which are activated at the time it takes for every load to travel the distance from the origin to every node's location. This is a more natural and realistic way to model vehicular load than by assuming the loads to be stationary or move quasi-statically without taking inertia effects into account.

Results from the present inelastic analyses are compared with elastic ones obtained in [4] and an assessment of the inelastic effects on the pavement response is made.

## 2 FEM MODELING IN SPACE AND TIME

This section deals with the finite element modeling of the pavement structure, the modeling of the moving vehicle loads and the finite element solution in the time domain. The first two subsections actually represent a summary of two full sections in [4] and are described here for reasons of completeness. The third subsection is an extension of the time domain solution from the elastic [4] to the present inelastic case.

### 2.1 Finite element modeling of pavement structure

The typical three dimensional (3-D), three layer flexible road pavement structure model used in [4] under conditions of linear elastic material behavior and shown in Fig.1 is adopted here for the present inelastic analyses. The model has dimensions 29.45m along the vertical z direction, 15.00m along the lateral (transverse) y direction and 30.00m along the longitudinal x direction and is supported in general by a deformable soil. It consists of three layers fully bonded to each other and to the supporting soil with the top one being the asphalt concrete layer of thickness 0.15m, the intermediate one the granular base layer of thickness 0.30m and the bottom one the subgrade layer of thickness 29.00m. The above pavement structure is discretized into a finite number of 8-noded 3-D solid elements (bricks) with 24 in total degrees of freedom (SOLID 185 type in ANSYS [20] program). The finite element mesh consists of 145920 elements or 155961 nodes ( $3 \times 155961 = 467883$  d.o.f.).

The above model is supported at its bottom and its lateral faces by rollers since, as it was found in [4] for the chosen domain and its discretization, this kind of boundary conditions gives almost the same high accuracy results with those obtained by using absorbing boundaries, at least for linear elastic material behaviour, provided a suitable time step has been chosen. It should be noticed that the lateral face of the model designated by the zx plane is a plane of symmetry and that the x axis represents the axis of the road pavement (Fig. 1).

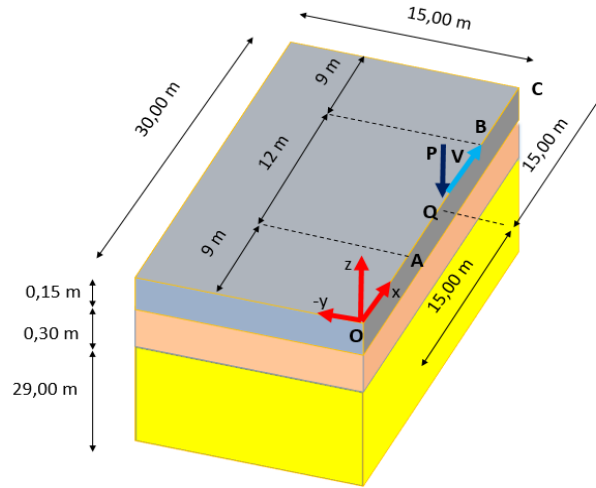


Figure 1: The three layered road pavement structure

## 2.2 Modeling of the moving vehicle loads

The typical heavy vehicle of 80kN used for the linear elastic analyses in [4], is also used here in its distributed load form, which is actually a superposition of closely spaced point or concentrated loads. The motion of a point load with constant speed along the x axis from point A to point B (Fig.1) is simulated by assigning time dependent load values at all the nodes of the line segment AB, which are activated at the time it takes for the load to travel the distance from A to every other node along AB. For more details one can consult [4]. As explained in [4], the point load  $P=80\text{kN}$  acts over an area of length 0.45m and width 0.30m and the resulting distributed load  $p=0.5926\text{ MPa}$  is converted into an equivalent system of point loads placed symmetrically on either side of x axis. These loads are treated as series of point loads parallel to the x axis for which their effect can be taken as a superposition of single point loads. Use is made of 28 axles of loads moving along the x axis for an almost perfect simulation. One should notice that because of symmetry, only half of those loads are utilized.

## 2.3 Finite element solution in time domain

Following standard finite element procedures [21], one can formulate the equation of motion of the pavement structure of Fig.1 as

$$[M]\{\ddot{u}\} + \{R(u, \dot{u}, \ddot{u})\} = \{F\} \quad (1)$$

where  $[M]$  is the mass matrix,  $\{u\}$  and  $\{F\}$  are the vectors of nodal displacements and nodal external forces respectively,  $\{R\}$  is the vector of the nodal internal resistance forces, which are nonlinear functions of  $\{u\}$ ,  $\{\dot{u}\}$  and  $\{\ddot{u}\}$  and overdots denote differentiation with respect to time  $t$ . Internal resistance forces  $\{R\}$  for linear elastic material behaviour, reduce to  $[K]\{u\}$ , where  $[K]$  is the stiffness matrix. External forces in  $\{F\}$  refer to nodes at the surface  $z=0$  of the pavement structure and come from the moving loads.

The step-by-step time integration algorithm of Newmark [21] of the constant acceleration type under zero initial conditions is used in this work to solve Eq. (1), as for the case of linear elastic material behavior. However, because of the non-linear character of Eq. (1) due to the presence of  $\{R\}$ , iterations are needed at every time step, which are performed with the aid of the modified Newton-Raphson scheme [21]. The above described solution procedure is done in the framework of the computer program ANSYS [20].

The selection of an appropriate value for the time step  $\Delta t$  to be used for the above time solution procedure in order to achieve stability and acceptable accuracy, is based on the rules established for the linear elastic case [21, 4]. Thus, on the basis of extensive studies done in [4] for the linear elastic case, a value of  $\Delta t = 0.3 \cdot 10^{-3}$  secs is selected here as a starting one for convergence studies.

### 3 MODELING THE MATERIAL BEHAVIOR OF LAYERS

This section briefly describes the three types of inelastic material behavior assumed for the three layers of the pavement structure of Fig.1. These are linear viscoelastic, elastoplastic and viscoplastic. Strictly speaking, linear viscoelasticity is not included in inelasticity, which implies nonlinearity. However, the term inelasticity is used here in the sense of non-elasticity and in that sense includes viscoelasticity. The following brief descriptions of material behavior come from [20, 22].

#### 3.1 Elastoplasticity

Elastoplastic isotropic material behavior can be of the von Mises (V.M.) or the Drucker-Prager (D-P) type, which is more appropriate for granular soil materials. The von Mises model is characterized by the elastic modulus  $E$ , the Poisson's ratio  $\nu$  and the yield stress  $\sigma_y$ , while the D-P model by  $E$ ,  $\nu$ , the internal friction angle  $\theta$ , the cohesion  $c$  given as

$$c = \sqrt{3} (3 - \sin\theta) \sigma_y / 6 \cos\theta \quad (2)$$

and the dilatancy angle  $\theta_f$  that describes the flow potential (non-associative case).

The V.M. and the D-P models have yield surfaces in the principal stress space in the form of a cylinder and a cone, respectively. In general, the yield surface is expressed as

$$F(\sigma, \kappa) = 0 \quad (3)$$

where  $\sigma$  is the stress tensor and  $\kappa$  the plastic work. In plasticity one works with increments or rates of stress  $\sigma$  and  $\epsilon$  strain tensors. Assuming associated plasticity one can express the plastic strain rate  $\dot{\epsilon}^p$  as

$$\dot{\epsilon}^p = \dot{\lambda} \frac{\partial F}{\partial \sigma} \quad (4)$$

where  $\dot{\lambda}$  is a constant to be determined. Indeed differentiating Eqn. (3) and taking into account that  $\dot{\kappa} = \sigma^T \dot{\epsilon}^p$  one receives

$$\frac{\partial F}{\partial \sigma} \dot{\sigma} + \frac{\partial F}{\partial \sigma} \sigma^T \dot{\epsilon}^p \quad (5)$$

Furthermore, one assumes that

$$\dot{\epsilon} = \dot{\epsilon}^e + \dot{\epsilon}^p \quad (6)$$

where  $\dot{\epsilon}$  and  $\dot{\epsilon}^e$  are the total strain rate and elastic strain rate, respectively. Invoking Hooke's law for the elastic strain rate and Eqs (4) and (6) one has

$$\dot{\sigma} = D \dot{\epsilon}^e = D \dot{\epsilon} - D \dot{\lambda} \frac{\partial F}{\partial \sigma} \quad (7)$$

where  $D$  is the elasticity matrix. Combining Eqs (4) - (7) one can determine  $\dot{\lambda}$  as

$$\dot{\lambda} = \frac{(\frac{\partial F}{\partial \sigma}) / D \dot{\epsilon}}{-\left(\frac{\partial F}{\partial \kappa}\right) \sigma^T \left(\frac{\partial F}{\partial \sigma}\right) + \left(\frac{\partial F}{\partial \sigma}\right)^T D \left(\frac{\partial F}{\partial \sigma}\right)} \quad (8)$$

and hence express  $\dot{\sigma}$  from (7) in the form

$$\dot{\sigma} = D^{ep} \dot{\epsilon} \quad (9)$$

where  $D^{ep}$  is the elastoplastic matrix.

### 3.2 Viscoplasticity and Viscoelasticity

Viscoplastic (VP) material behavior is usually assigned to the asphalt layer of the pavement structure of Fig.1. Viscoplasticity combines viscous and plastic material behavior and appears to be the ideal theory for describing asphalt material behavior. According to the viscoplastic model of Perzyna [20] adopted in this work, the viscoplastic strain rate tensor  $\dot{\epsilon}^{vp}$  is given by

$$\dot{\epsilon}^{vp} = \gamma \left( \frac{\sigma}{\sigma_y} - 1 \right)^{1/m} \quad (10)$$

where  $\gamma$  is the material viscosity parameter in  $(\text{sec})^{-1}$ ,  $\sigma$  is the equivalent stress,  $\sigma_y$  is the (static) yield stress of the material and  $m$  is the strain rate hardening parameter. The above  $\dot{\epsilon}^{vp}$  plays the role of  $\dot{\epsilon}^p$  in elastoplasticity of subsection 3.1, which is valid here as well. One can use the above viscoplastic model to approximately simulate viscoelastic (VE) behavior on the assumption that  $\sigma_y \rightarrow \infty$  (practically a very large value).

## 4 NUMERICAL RESULTS

The moving load path for the case of linear elastic material behavior of the pavement layers was segment (AB) = 12.00m of Fig.1, while the time step for convergent results was  $\Delta t = 0.3 \cdot 10^{-3}$  secs. However, for the present non-linear material behavior case, convergent results required a time step  $\Delta t = 0.15 \cdot 10^{-3}$  secs resulting in very large computational times. For this reason, the moving load path for this case was reduced to a segment (A'B') = 3.60m with its middle being also point Q (Fig.1). The distributed load  $p = 0.5926$  MPa moves along the x axis (Fig.1) with a constant speed of 20 m/s (72 km/h).

Consider the three layers domain of Fig.1 with the following material properties:  $E_1=1000$  MPa,  $\nu_1=0.35$ ,  $\rho_1=2500$  kg/m<sup>3</sup> for the top layer,  $E_2=400$  MPa,  $\nu_2=0.35$ ,  $\rho_2=2100$  kg/m<sup>3</sup> for the intermediate layer and  $E_3=80$  MPa,  $\nu_3=0.40$ ,  $\rho_3=2000$  kg/m<sup>3</sup> for the bottom layer, where  $E, \nu$  and  $\rho$  denote modulus of elasticity, Poisson's ratio and mass density, respectively. On the basis of this three layers system the following inelastic models are considered:

- 1) Top layer V.M. elastoplastic with yielding stress  $\sigma_y = 188.50 \cdot 10^3$  Pa and the other two layers elastic.
- 2) All layers V.M. elastoplastic with yielding stress  $\sigma_{y1} = 188.50 \cdot 10^3$  Pa,  $\sigma_{y2} = 94.25 \cdot 10^3$  Pa,  $\sigma_{y3} = 62.83 \cdot 10^3$  Pa.
- 3) Top layer viscoelastic as a special case of Perzyna's viscoplastic model ( $\sigma_y = 500$ MPa,  $\gamma = 0.1 \text{ sec}^{-1}$ ,  $m=0.01$ ) and the other two layers elastic.
- 4) Top layer viscoplastic with  $\gamma=10^{-4} \text{ sec}^{-1}$ ,  $m=0.28$  and  $\sigma_y=350$ kPa and the other two layers elastic.
- 5) Top layer viscoplastic as in case 4) and the other two elastoplastic of the D-P type with  $\sigma_y=225.15$ kPa,  $\theta=40^\circ$ ,  $\theta_f=13^\circ$  and  $\sigma_y=30.217$ kPa,  $\theta=28^\circ$ ,  $\theta_f=9^\circ$  for second and third layer, respectively.

Figures 2 and 3 display the time history of the vertical displacement and vertical stress at the bottom of the top layer for Model 1. For comparison reasons, results for the case of all the layers being elastic (Model 0) are also provided. It is observed that inelasticity increases the maximum value of displacement and decreases that of the stress.

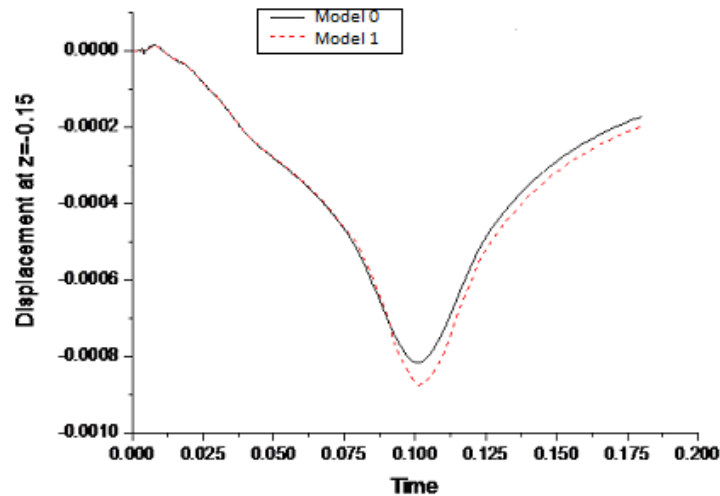


Figure 2: Time history of vertical displacement at  $z=-0.15$ m for Model 1

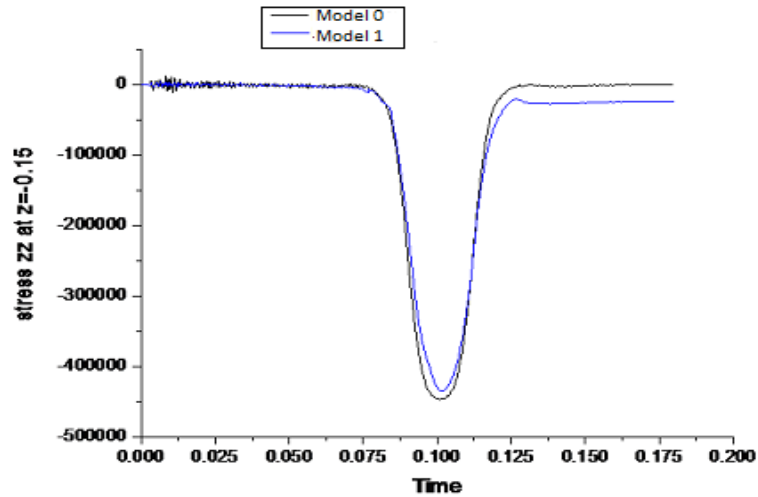


Figure 3: Time history of vertical stress at  $z=-0.15\text{m}$  for Model 1

Figures 4 and 5 display the time histories of the vertical displacement and vertical stress at the bottom of the top layer for Model 2. It is observed again that inelasticity increases the maximum value of displacement and decreases that of the stress. In this particular case, the results for the displacement are unrealistically high because all the layers are elastoplastic and the values of  $\sigma_y$  are very low.

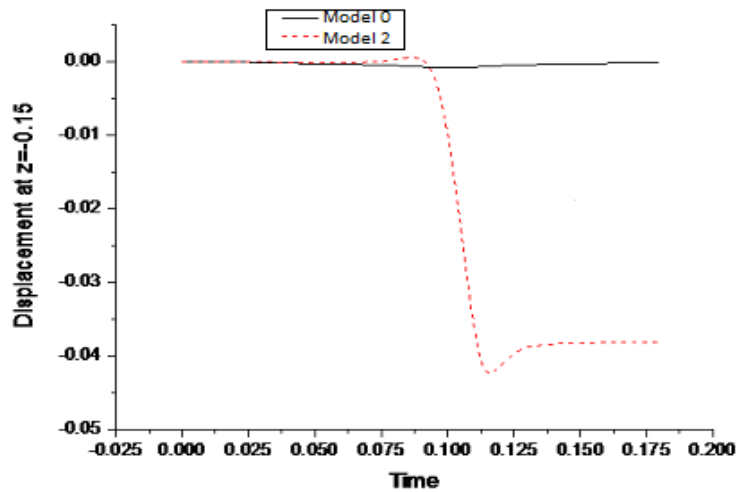


Figure 4: Time history of vertical displacement at  $z=0.15\text{m}$  for Model 2

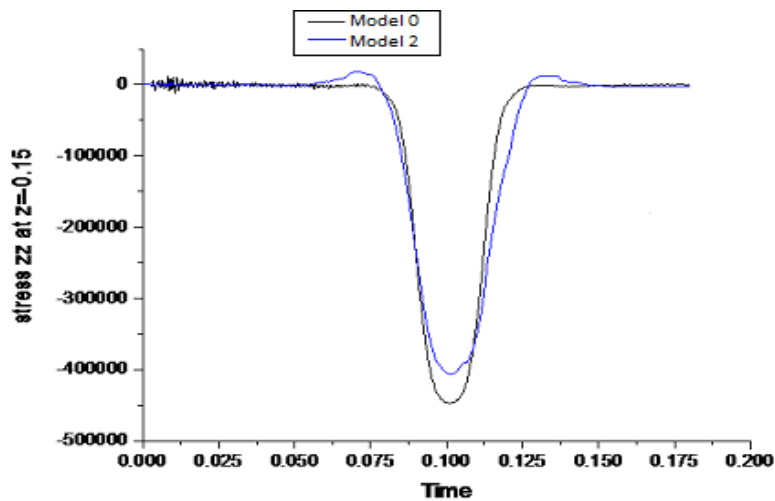


Figure 5: Time history of vertical stress at  $z=-0.15\text{m}$  for Model 2

Figures 6 and 7 depict the time histories of the vertical displacement and vertical stress at the bottom of the top layer for Model 3. For comparison purposes, results for the case of all the layers being elastic (Model 0) are also provided. It is observed that viscous effects, at least for the material parameters selected here, are negligible.

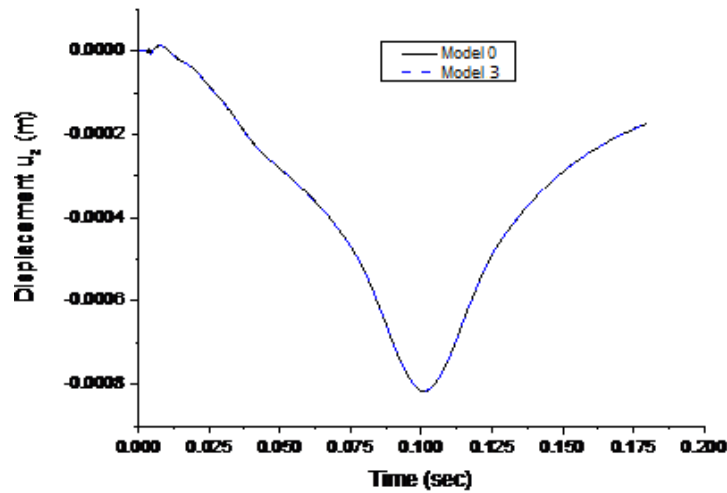


Figure 6: Time history of vertical displacement at  $z=-0.15\text{m}$  for Model 3

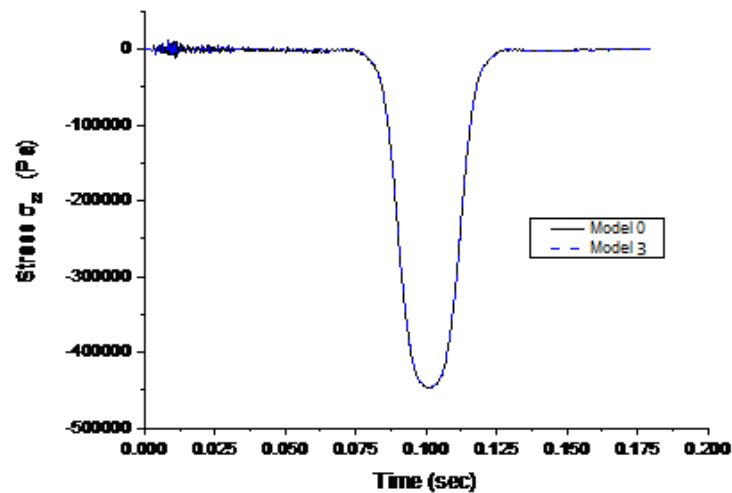


Figure 7: Time history of vertical stress at  $z=-0.15\text{m}$  for Model 3

Figures 8 and 9 show the time histories of the vertical displacement and vertical stress at the bottom of the top layer for Model 4. Results for the purely elastic case (Model 0) are also shown there. It is observed that, while the maximum displacement is not affected by inelasticity, the maximum stress decreases because of that.

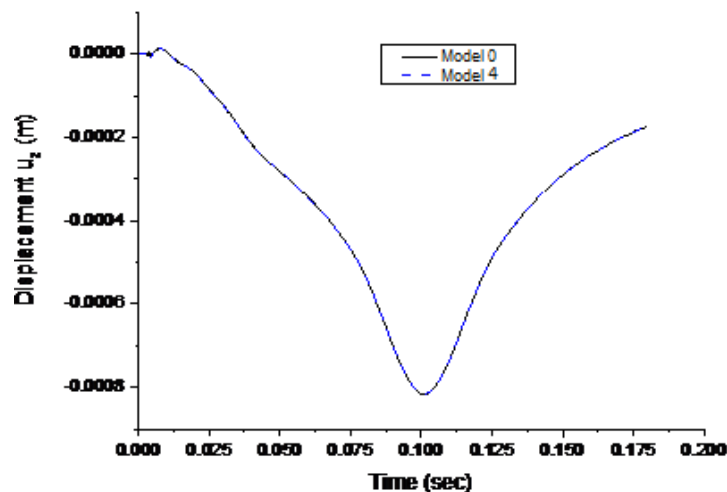


Figure 8: Time history of vertical displacement at  $z=-0.15\text{m}$  for Model 4

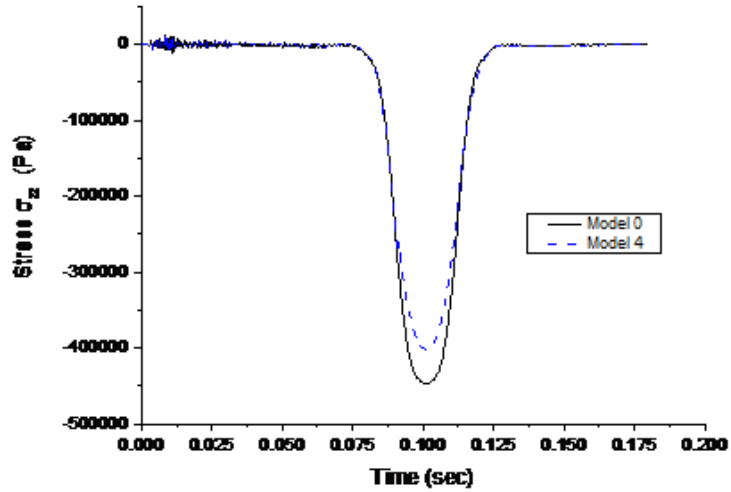


Figure 9: Time history of vertical stress at  $z=-0.15\text{m}$  for Model 4

Figures 10 and 11 show the time histories of the vertical displacement and vertical stress at the bottom of the top layer for Model 5. Results for the purely elastic case (Model 0) are also shown there. It is observed that, while the maximum displacement is not affected by inelasticity, the maximum stress decreases because of that.

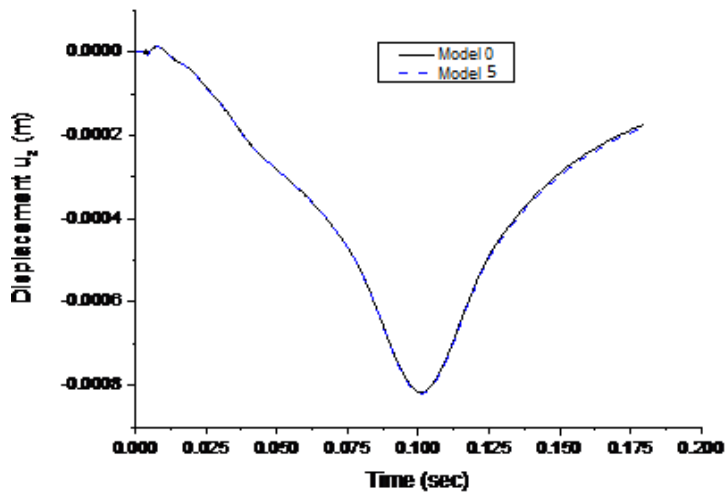


Figure 10: Time history of vertical displacement at  $z=-0.15\text{m}$  for Model 5

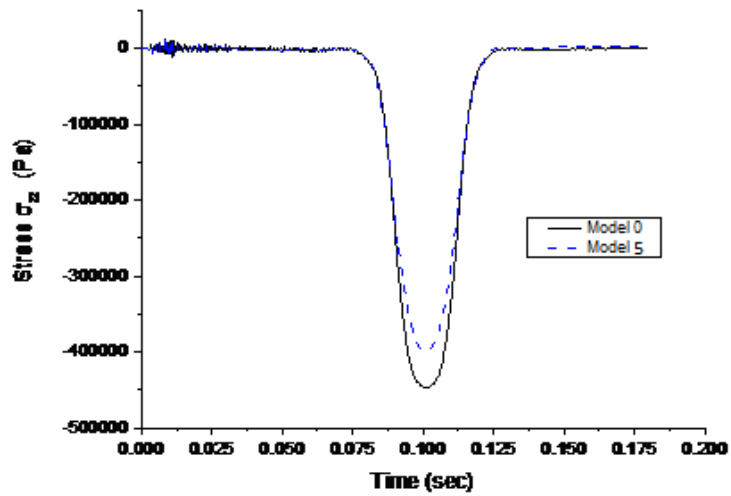


Figure 11: Time history of vertical stress at  $z=-0.15\text{m}$  for Model 5

## 5 CONCLUSIONS

On the basis of the preceding developments, one can draw the following conclusions:

- 1) A general three-dimensional model for the simulation in the time domain of the dynamic response of a flexible three layers road pavement to the motion of a vehicle, constructed in the framework of the ANSYS computer program, has been extended from the case of linear elastic material behavior to that of inelastic one.
- 2) Five inelastic models have been considered: One with the top layer being elastoplastic of the V.M. type and the other two elastic, one with all three layers being elastoplastic of the V.M. type, one with the top layer being viscoelastic and the other two elastic, one with the top layer being viscoplastic and the other two elastic and one with the top layer being viscoplastic and the other two elastoplastic of the D-P type.
- 3) In all cases considered here, the maximum values of the vertical displacements and stresses at the bottom of the top layers have been determined and compared with the corresponding ones under elastic behavior in all layers. It was found that inelasticity slightly increases displacements and decreases stresses.
- 4) More work is required to produce more detailed results for all the models considered here, study the cases of other vehicle speeds and compare elastic and inelastic results against those coming out of experiments.

## ACKNOWLEDGEMENT

The first author (Niki D.Beskou) acknowledges with thanks the support provided to her by the 'IKY fellowships of excellence for postgraduate studies in Greece-Siemens program'. All the authors acknowledge with thanks helpful discussions with Professor S.V.Tsinopoulos.

## REFERENCES

- [1] Huang, Y.H. (2004), '*Pavement Analysis and Design*', Pearson Prentice-Hall, Upper Saddle River, New Jersey, USA.
- [2] Beskou, N.D., Theodorakopoulos, D.D. (2011), '*Dynamic effects on moving loads on road pavements: A review*', Soil Dynamics and Earthquake Engineering 31, pp.547-567.
- [3] Monismith, C.L. (2012), '*Flexible pavement analysis and design-A half century of achievement*', Geotechnical Engineering State of the Art and Practice, GSP 226, K.Rollins and D.Zekkos, Editors, ASCE, pp. 187-220.
- [4] Beskou, N.D., Tsinopoulos, S.V., Theodorakopoulos, D.D. (2015), '*Finite element elastic analysis of 3-D flexible pavements under moving loads*', Proceedings of COMPDYN 2015, Crete, Greece, 25-27 May 2015.
- [5] Elseifi, M.A., Al-Quadi, I.L., Yoo, P.J. (2006), '*Viscoelastic modeling and field validation of flexible pavements*', Journal of Engineering Mechanics of ASCE 132 (2), pp.172-178.
- [6] Liao, J., Sargand, S. (2010), '*Viscoelastic FE modeling and verification of a U.S. 30 perpetual pavement test section*', Road Materials and Pavement Design 11, pp.993-1008.
- [7] Khavassefat, P., Jelagin, D., Birgisson, B. (2012), '*A computational framework for viscoelastic analysis of flexible pavements under moving loads*', Materials and Structures 45, pp.1655-1671.
- [8] Duncan, J.M., Monismith, C.L., Wilson, E.L. (1968), '*Finite element analyses of pavements*', Highway Research Record 228, pp.18-33.
- [9] Elliott, R.P., Thompson, M.R. (1985), '*ILLI-PAVE mechanistic analysis of AASHO road test flexible pavements*', Transportation Research Record 1043, pp.33-49.
- [10] Harichandran, R.S., Yeh, M.S., Baladi, G.Y. (1990), '*MICH-PAVE: A nonlinear finite element program for analysis of flexible pavements*', Transportation Research Record 1286, pp.123-131.
- [11] Chen, D.H., Zaman, M., Laguros, J.G., Soltani, A. (1995), '*Assessment of computer programs for analysis of flexible pavement structure*', Transportation Research Record 1482, pp.123-133.
- [12] Guezouli, S., Elhannani, M., Jouve, P. (1996), '*NOEL: a nonlinear finite element code for road pavement analysis*', in Flexible Pavements, Gomes Correias, A., Editor, A.A. Balkema, Rotterdam, pp. 193-200.
- [13] Helwany, S., Dyer, J., Leidy, J. (1998), '*Finite-element analyses of flexible pavements*', Journal of Transportation Engineering of ASCE 124 (5), pp.491-499.
- [14] Al-Qadi, I.L., Wang, H., Tutumluer, E. (2010), '*Dynamic analysis of thin asphalt pavements by using cross-anisotropic stress-dependent properties for granular layer*', Transportation Research Record 2154, pp.156-163.
- [15] Zaghoul, S., White, T. (1993), '*Use of a three-dimensional, dynamic finite element program for analysis of flexible pavements*', Transportation Research Record 1388, pp.60-69.

- [16] Sukumaran, B., Chamala, N., Willis, M., Davis, J., Jurewicz, S., Kyatham, V. (2004), '*Three-dimensional finite element modeling of flexible pavements*', Proceedings of 2004 FAA Worldwide Airport Technology Transfer Conference, Atlantic City, N.J., USA, April 2004.
- [17] Saad, B., Mitri, H., Poorooshab, H. (2005), '*Three-dimensional dynamic analysis of flexible conventional pavement foundation*', Journal of Transportation Engineering of ASCE 131 (6), pp.460-469.
- [18] Fang, H., Hand, A.J., Haddock, J.E., White, T.D. (2007), '*An object-oriented framework for finite element pavement analysis*', Advances in Engineering Software 38, pp.763-771.
- [19] Ali, B., Sadek, M., Shahrour, I. (2008), '*Elasto-visco-plastic finite element analysis of the long-term behavior of flexible pavements*', Road Materials and Pavement Design 9, pp.463-479.
- [20] ANSYS, (2000), ANSYS LS-DYNA User's Guide, Release 13, ANSYS Inc. Southpointe, Canonsburg, PA, USA.
- [21] Bathe, K.J. (1996), '*Finite Element Procedures*', Prentice-Hall, Englewood Cliffs, New Jersey.
- [22] Zienkiewicz, O.C., Taylor, RL (2000), '*The Finite Element Method; Vol.2: Solid Mechanics*', 5<sup>th</sup> edition, Butterworth-Heinemann, London.